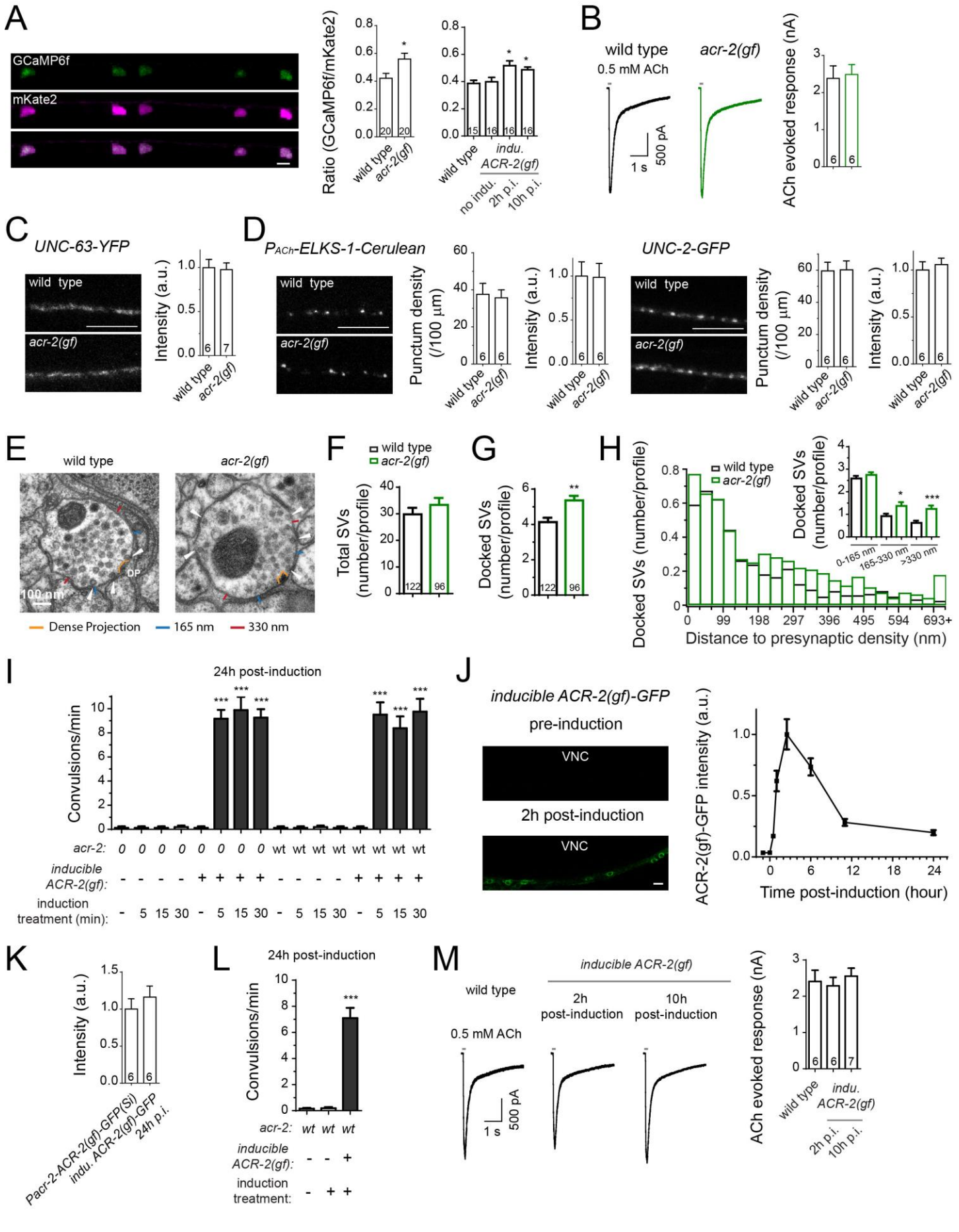
A
GCaMP6f
mKate2
Ratio (GCaMP6f/mKate2)
wild type
acr-2(gf)
indu. ACR-2(gf)
no indu.
2h p.i.
10h p.i.
B
wild type
0.5 mM ACh
acr-2(gf)
500 pA
1 s
ACh evoked response (nA)
C
UNC-63-YFP
wild type
acr-2(gf)
Intensity (a.u.)
D
PACh-ELKS-1-Cerulean
UNC-2-GFP
Punctum density (/100 µm)
E
wild type
acr-2(gf)
DP
100 nm
Dense Projection
165 nm
330 nm
F
Total SVs (number/profile)
G
Docked SVs (number/profile)
H
Docked SVs (number/profile)
Distance to presynaptic density (nm)
0-165 nm
165-330 nm
>330 nm
I
24h post-induction
Convulsions/min
acr-2:
inducible ACR-2(gf):
induction treatment (min):
J
inducible ACR-2(gf)-GFP
pre-induction
VNC
2h post-induction
ACR-2(gf)-GFP intensity (a.u.)
Time post-induction (hour)
K
Pacr-2-ACR-2(gf)-GFP(Si)
indu. ACR-2(gf)-GFP
24h p.i.
L
24h post-induction
M
inducible ACR-2(gf)
wild type
2h post-induction
10h post-induction
0.5 mM ACh
indu. ACR-2(gf)
2h p.i.
10h p.i.

Figure S1. Synaptic morphology in *acr-2(gf)* and inducible expression of ACR-2(gf), related to Figure 1

(A) Representative images of animals carrying *Pacr-2-GCaMP6f-SL2-mKate2* (left), ratio of GCaMP6f and mKate2 in wild type and *acr-2(gf)* (middle), and in animals with *inducible ACR-2(gf)* and wild type controls (right).

(B) Average traces (left) and mean amplitudes (right) of 0.5 mM ACh-evoked postsynaptic responses in wild type and *acr-2(gf)*.

(C) Representative images and intensity of *UNC-63-YFP* (*kr98*) in wild type and *acr-2(gf)*. Intensities are normalized to wild type.

(D) Representative images, punctum density and intensity of *Punc-129-ELKS-1-Cerulean* (*tauIs12*) (left) and UNC-2-GFP (vaIs33) (right) in wild type and *acr-2(gf)*. Intensities are normalized to wild type.

(E) Representative EM images of ultrastructural organization of cholinergic neuromuscular junctions in wild type and *acr-2(gf)* mutants. EM data were collected from one wild type animal (21 synapses, 122 profiles and 501 docked synaptic vesicles) and one *acr-2(gf)* animal (20 synapses, 96 profiles and 525 docked synaptic vesicles).

(F-G) The average number of total SVs (F) and docked SVs (G) in single profiles of cholinergic synapse containing a dense projection in wild type and *acr-2(gf)*.

(H) Histogram of docked vesicle number per profile located at different distances to the presynaptic dense projection in wild type and *acr-2(gf)*. Insert, the average docked vesicle number per profile from each synapse in specific regions (<165 nm, 165-330 nm and >330 nm).

(I) Convulsion rates 24 hours post-induction with different induction times of heat shock treatment in *inducible ACR-2(gf)* animals. n=8 for each conditions. L4 stage animals were treated with heat shock.

(J) Representative images of inducible ACR-2(gf)-GFP expression in ventral nerve cord (VNC) pre-induction or 2 hours post-induction (left) and time course of GFP intensities (n=5).

(K) GFP intensities of single copy insertion of ACR-2(gf)-GFP and inducible ACR-2(gf)-GFP expression 24 hours post-induction.

(L) Convulsion rates 24 hours post-induction of heat shock treatment in wild type and *inducible ACR-2(gf)* animals in indicated conditions. n=10 for each conditions. Adult stage animals were treated with heat shock.

(M) Average traces (left) and mean amplitude of 0.5 mM ACh-evoked postsynaptic responses from indicated genotypes and conditions in 1.2 mM Ca^{2+} bath solution. Data from wild type were recorded 2 hours post-induction treatment.

Scale bar: 5 m in (A), (C), (D) and (J). a.u. represents arbitrary unit. ***, $p<0.001$; **, $p<0.01$; *, $p<0.05$. Sample size is shown within each bar.

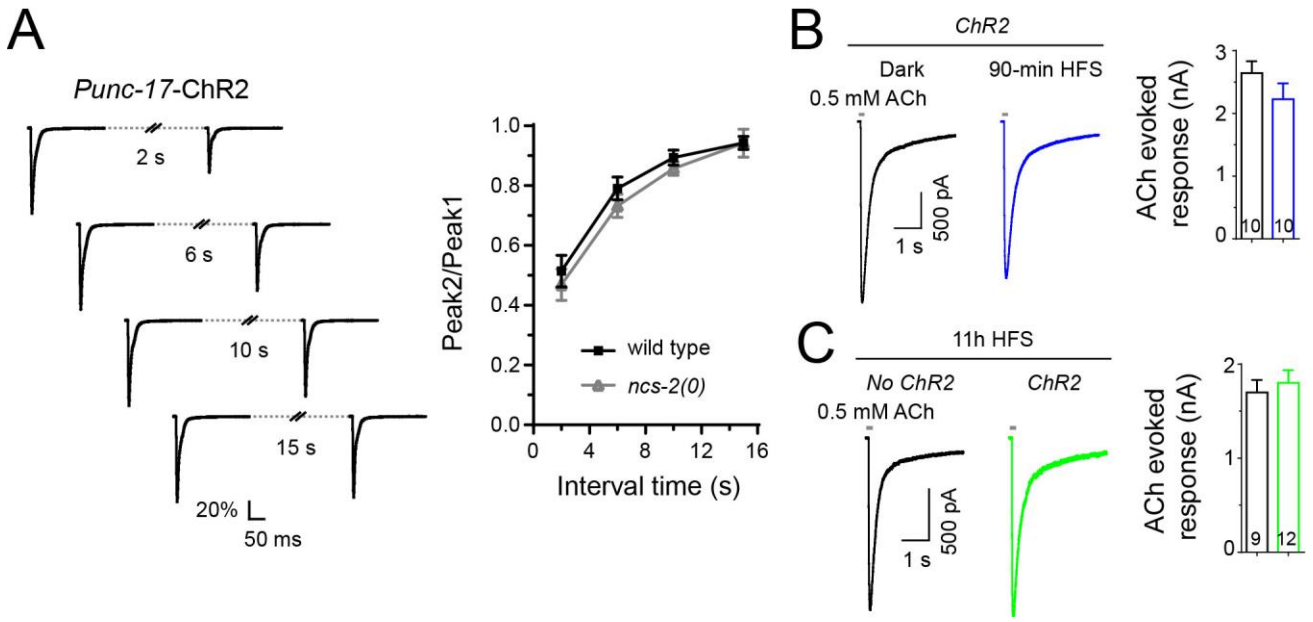

Figure S2. Recovery of eEPSCs with dual stimulation of *Punc-17-ChR* and postsynaptic responses to exogenous ACh, related Figure 2.

(A) Ration of eEPSC amplitudes with dual stimulation of *Punc-17-ChR2* by blue light in wild type (n=8) and *ncs-2(tm1943)* (n=8).
(B-C) Average traces (left) and mean amplitudes (right) of 0.5 mM ACh-evoked postsynaptic responses in animals under different conditions and treatments.
Sample size is shown within each bar.

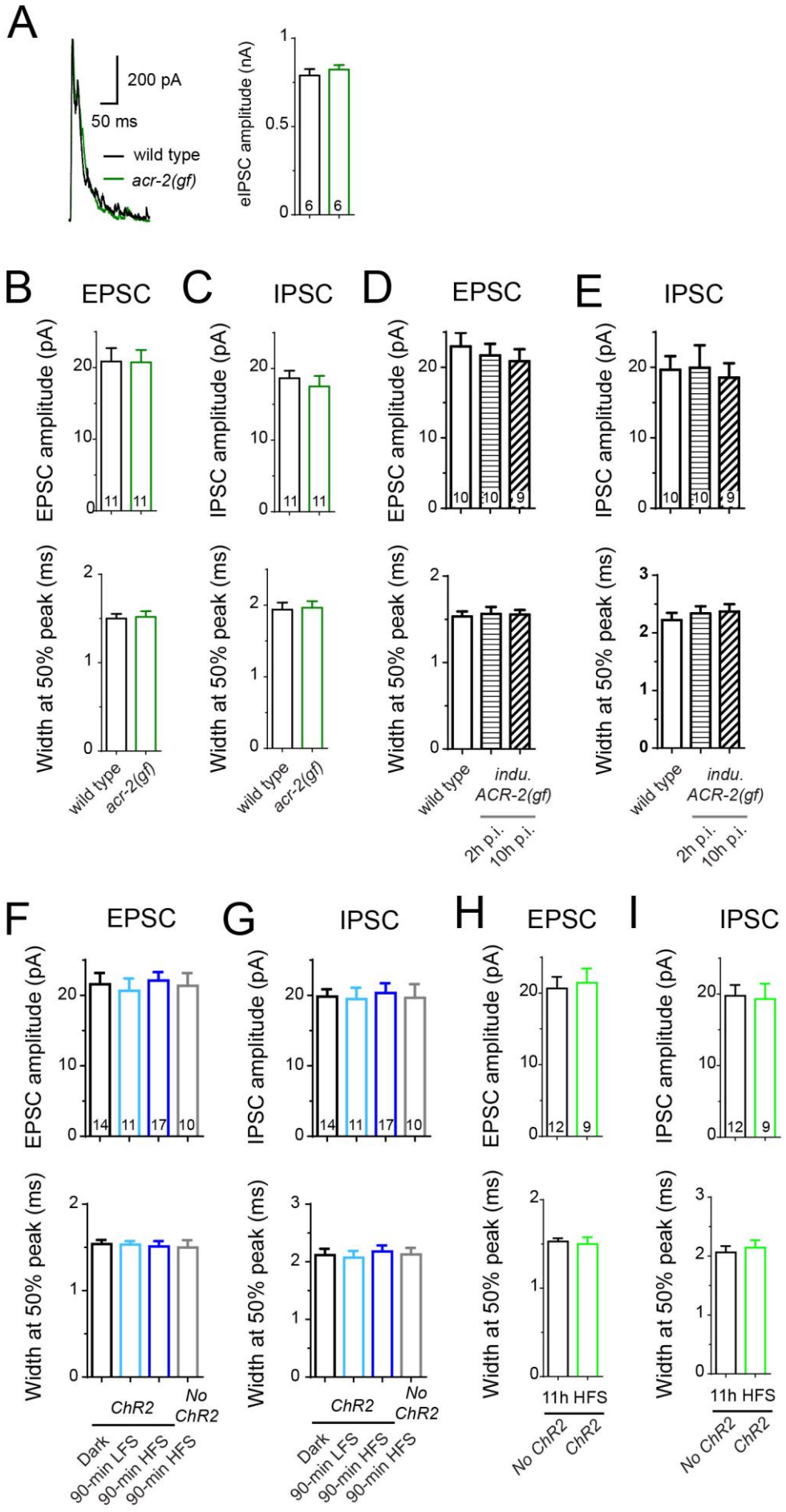
A
200 pA
50 ms
wild type
acr-2(gf)
eIPSC amplitude (nA)
B
EPSC
EPSC amplitude (pA)
Width at 50% peak (ms)
wild type
acr-2(gf)
C
IPSC
IPSC amplitude (pA)
D
EPSC
indu. ACR-2(gf)
2h p.i.
10h p.i.
E
IPSC
F
EPSC
ChR2
No ChR2
Dark
90-min LFS
90-min HFS
G
IPSC
H
EPSC
11h HFS
No ChR2
ChR2
I
IPSC

Figure S3. Evoked response in GABAergic neurons by stimulation of *Punc-47-ChR2*, and amplitude and kinetics of endogenous EPSC and IPSC in *acr-2(gf)* and ChR2-expressing animals, related to Figure 3

(A) Evoked inhibitory postsynaptic currents triggered by *Punc-47-ChR2* in wild type and *acr-2(gf)* mutants.

(B-C) Mean amplitudes and mean widths at 50% peak of endogenous EPSCs (B) and IPSCs (C) from wild type and *acr-2(gf)* in 2 mM Ca^{2+} bath solutions.

(D-E) Mean amplitudes and mean widths at 50% peak of endogenous EPSCs (D) and IPSCs (E) from indicated genotypes and conditions in 1.2 mM Ca^{2+} bath solutions.

(F-I) Mean amplitudes and mean widths at 50% peak of endogenous EPSCs (F and H) and IPSCs (G and I) from animals under different indicated genotypes and treatments in 2 mM Ca^{2+} bath solutions.

Sample size is shown within each bar.

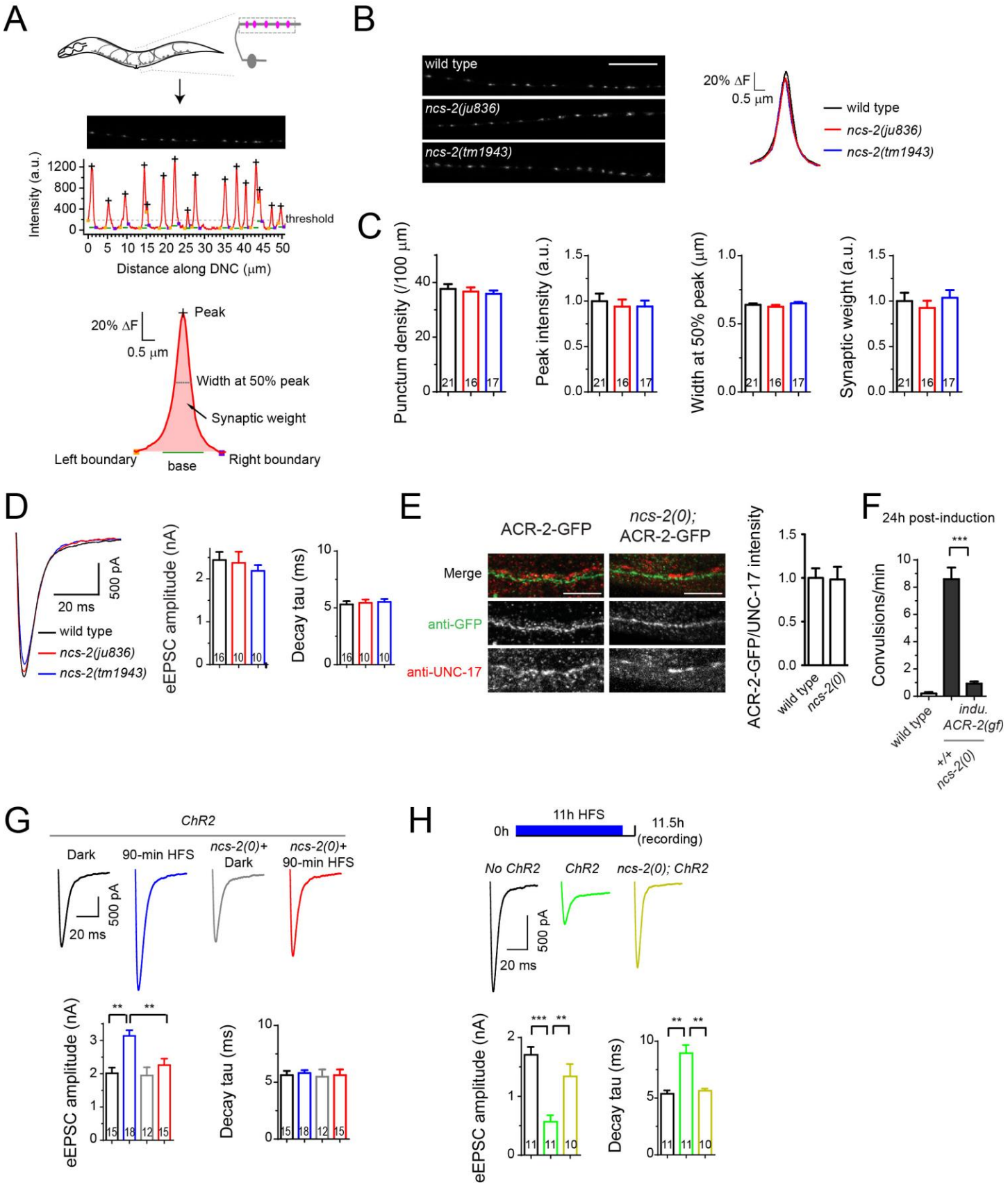

Figure S4. *ncs-2* mutants do not affect synaptic morphology and the baseline of synaptic transmission, related to Figure 4

(A) Illustration of fluorescent punctum analysis. Top panel: puncta representing synapses were located along dorsal nerve cord (DNC) of *C. elegans*. Middle panel: a linescan and analysis of punctum distribution for the above image. Bottom panel: single punctum with calculated parameters.
(B-C) Representative images, average shapes (B) and distribution (C) of puncta of *Punc-129-mCherry-RAB-3* (*tauIs46*) in indicated genotypes. Peak intensities and synaptic weights are normalized to wild type.
(D) Average traces (left), mean amplitude (middle) and mean decay tau (right) of eEPSCs from indicated genotypes in 1.2 mM Ca^{2+} bath solutions.
(E) ACR-2-GFP intensity normalized to UNC-17 intensity in wild type and *ncs-2(tm1943)*. n>10 for each genotypes.
(F) Convulsion rates in indicated genotypes and induction conditions. n = 10 for each genotypes.
(G-H) Average traces (top), mean amplitudes and mean decay tau (bottom) of eEPSCs from indicated genotypes and conditions in 2 mM Ca^{2+} bath solutions.
Scale bar: 10 μm in (B) and (E). a.u. represents arbitrary unit. ***, $p<0.001$; **, $p<0.01$. Sample size is shown within each bar.

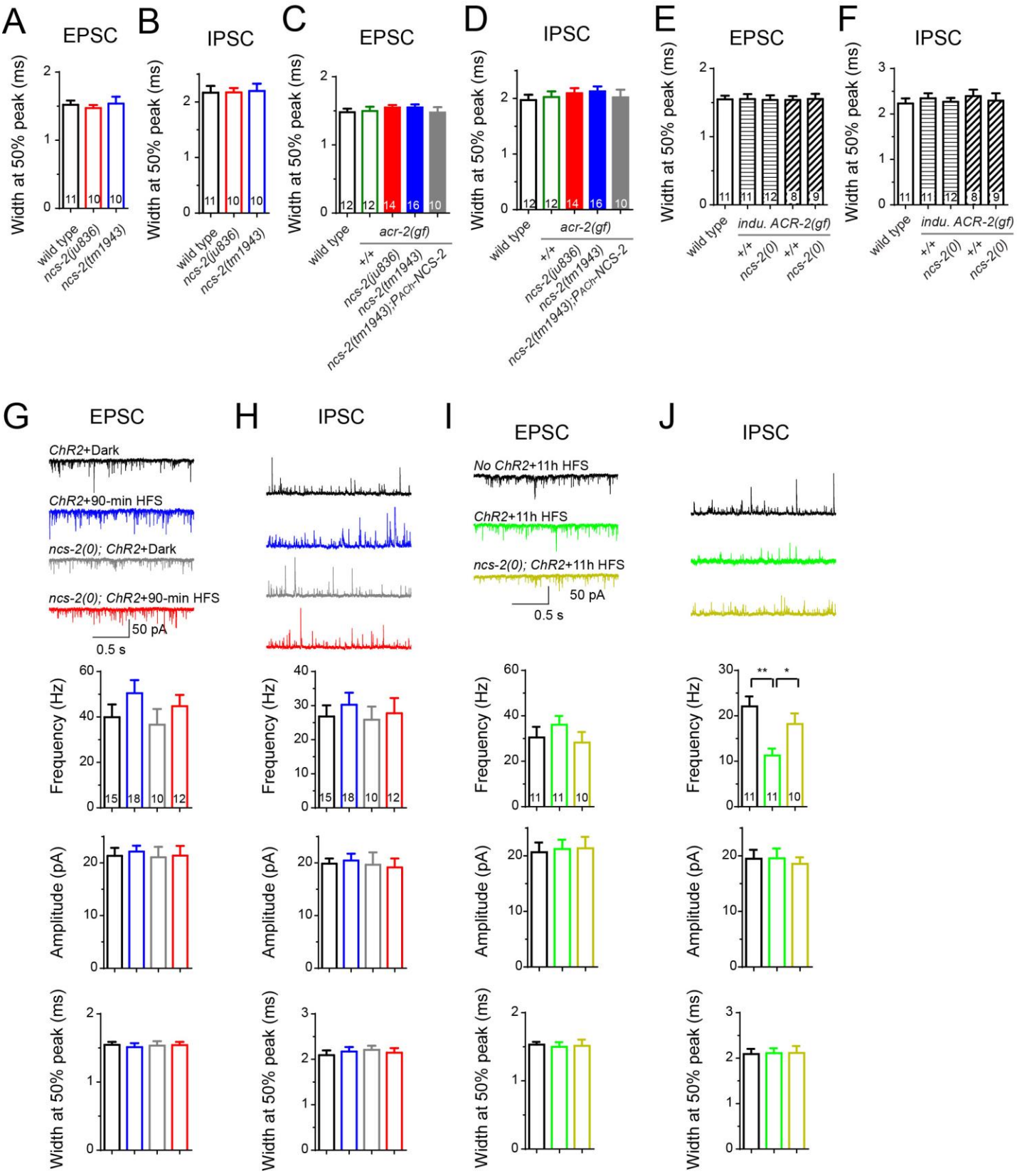

Figure S5. Effects of *ncs-2* mutants on endogenous EPSC and IPSC, related to Figure 5

(A-F) Mean widths at 50% peak of endogenous EPSCs and IPSCs from indicated genotypes and conditions.

(G-J) Representative traces, mean frequencies, mean amplitudes and mean widths at 50% peak of endogenous EPSCs (G and I) and IPSCs (H and J) from indicated genotypes and conditions in 2 mM Ca^{2+} bath solutions.

Sample size is shown within each bar.

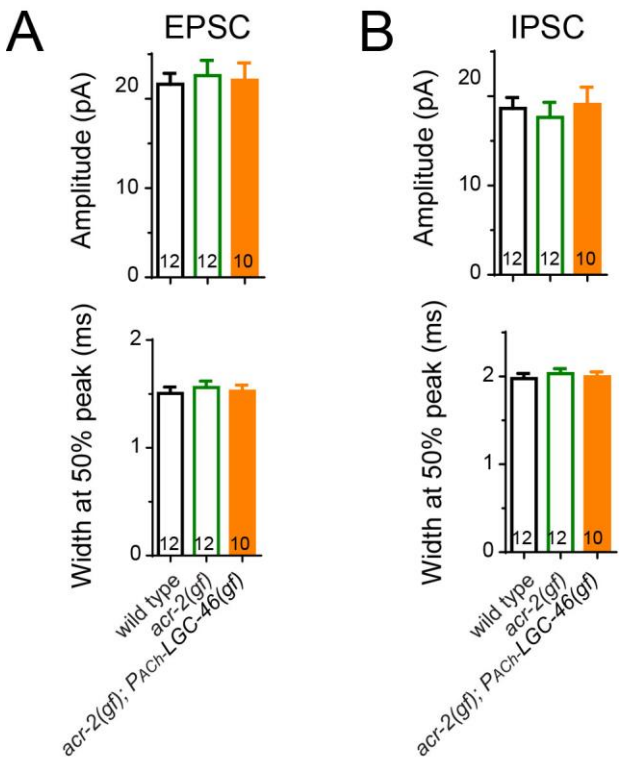

Figure S6. LGC-46(gf) has not effects on kinetics of endogenous EPSCs and IPSCs, related to Figure 6
(A-B) Mean amplitudes and mean widths at 50% peak of endogenous EPSCs (A) and IPSCs (B) from indicated genotypes in 2 mM Ca^{2+} bath solutions.

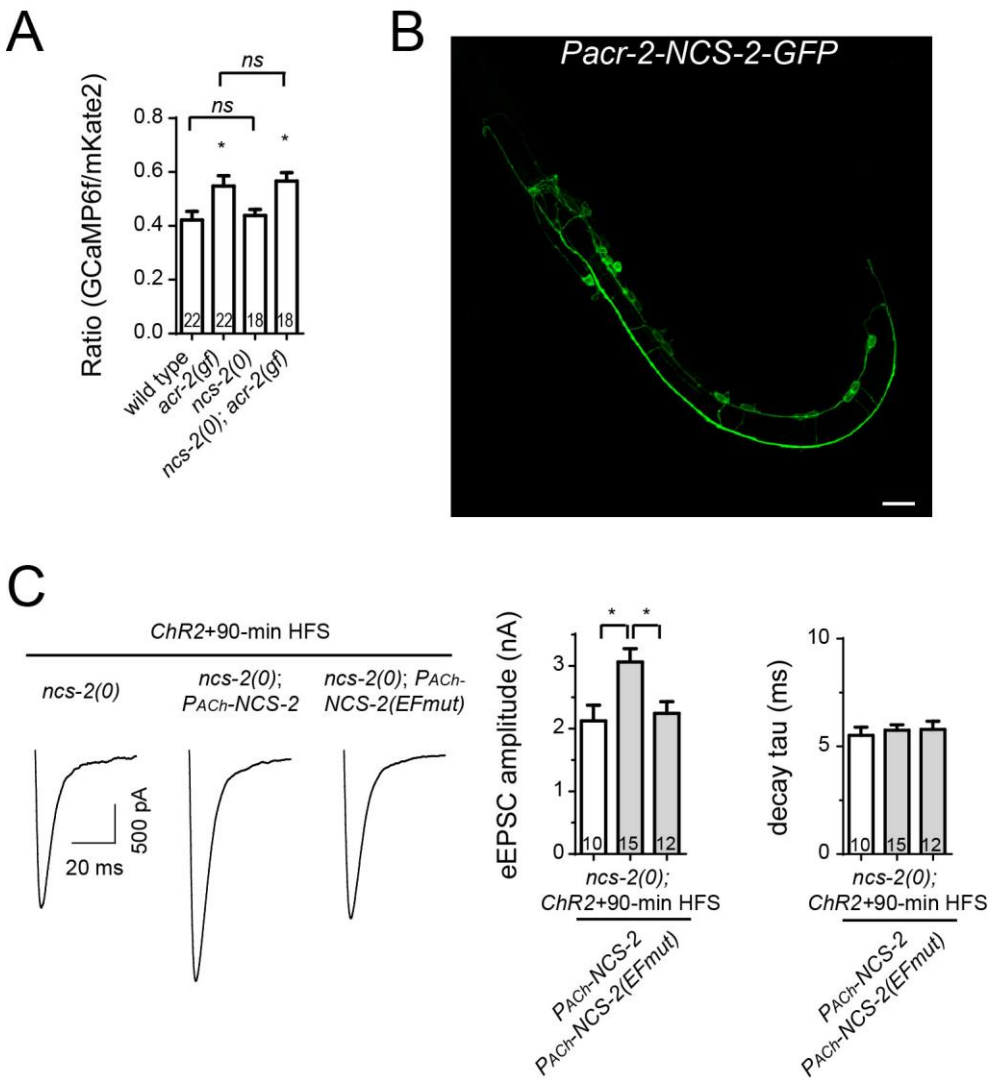

Figure S7. *ncs-2* mutants do not affect basal Ca^{2+}, related to Figure 7

(A) Ratio of GCaMP6f and mKate2 in indicated genotypes.

(B) NCS-2-GFP driven by *Pacr-2* is expressed in both somatodendrites and axonal processes at L1 stage after hatch. Scale bars: 10 µm.

(C) eEPSCs in indicated genotypes and conditions.

*, $p<0.05$. Sample size is shown within each bar.

Supplemental Tables

Table S1. Strain information, related to Figure 1-7

Strain	Genotype	Allele description, and notes
N2	wild type	
CZ10402	*acr-2(n2420) X*	*n2420*: g4944a (V309M) in K11G12.2 (Jospin et al., 2009)
JSD25	*tauIs12[Punc129-ELKS-1-Cerulean]*	Previously reported in (Martin et al., 2011)
CZ20048	*acr-2(n2420) X; tauIs12[Punc129-ELKS-1-Cerulean]*	
EN98	*unc-63[kr98-YFP] I*	UNC-63-YFP knock in at the endogenous locus (Gendrel et al., 2009)
CZ24849	*unc-63[kr98-YFP] I; acr-2(n2420) X*	
CZ21294	*unc-63[kr98-YFP] ncs-2(tm1943) I*	UNC-63-YFP is not altered in *ncs-2(tm1943)*
CZ20473	*ncs-2(ju836) I*	*ju836*: c284t (R72Stop) in F10G8.5
CZ20427	*ncs-2(ju836) I; acr-2(n2420) X*	
CZ22071	*ncs-2(ju843) I; acr-2(n2420) X*	*ju843*: c17t (S6F) in F10G8.5
CZ20527	*ncs-2(tm1943) I*	*tm1943*: 1,001 bp deletion in F10G8.5, removes 5' sequences including 486 bp promoter sequences and the first two exons
CZ20212	*ncs-2(tm1943) I; acr-2(n2420) X*	
CZ22238	*nuIs321[Punc-17-mCherry]; juEx6719[Pncs-2-GFP]*	*ncs-2* transcriptional reporter is expressed in cholinergic neurons.
CZ22241	*juIs223[Pttr-39-mCherry]; juEx6719[Pncs-2-GFP]*	*ncs-2* transcriptional reporter is expressed in GABAergic neurons.
CZ22459	*juSi260[Pncs-2-NCS-2-GFP] ncs-2(tm1943) I*	Cas9-mediated insertion on Ch I (*ttTi4348*)
CZ22345	*juSi260[Pncs-2-NCS-2-GFP] ncs-2(tm1943) I; acr-2(n2420) X*	
CZ22648	*ncs-2(tm1943) I; acr-2(n2420) X; juEx6887[Prgef-1-NCS-2-GFP]*	multiple lines were visually observed for effects on *acr-2(gf)* induced behavior, and 2 lines were quantitated for convulsion frequency.
CZ21621	*ncs-2(tm1943) I; acr-2(n2420) X; juEx6574[Punc-17β-NCS-2]*	multiple lines were visually observed for effects on *acr-2(gf)* induced behavior, and 2 lines were quantitated for convulsion frequency.

CZ22652	*ncs-2(tm1943) I; acr-2(n2420) X; juEx6889[Punc-25-NCS-2-GFP]*	multiple lines were visually observed for effects on *acr-2(gf)* induced behavior, and 2 lines were quantitated for convulsion frequency.
CZ19997	*tauIs46[Punc129-mCherry-RAB-3]*	
CZ20528	*ncs-2(tm1943) I; tauIs46[Punc129-mCherry-RAB-3]*	
CZ20821	*ncs-2(ju836) I; tauIs46[Punc129-mCherry-RAB-3]*	
CZ13763	*Pacr-2-ACR-2-GFP(juSi21) II*	Mos1-mediated insertion on Ch II (*ttTi5605*) (Qi et al., 2013)
CZ21203	*ncs-2(tm1943) I; Pacr-2-ACR-2-GFP(juSi21) II*	
CZ19788	*lite-1(ce314) X*	
CZ23320	*lite-1(ce314) X; juIs489[Punc-17-ChetaHR-mKate2]*	
CZ22837	*ncs-2(tm1943) I; lite-1(ce314) X; juIs489[Punc-17-ChetaHR-mKate2]*	
CZ23338	*ncs-2(tm1943) I; lite-1(ce314) X; juIs489[Punc-17-ChetaHR-mKate2]; juEx7118[Pacr-2-NCS-2-GFP]*	
CZ23339	*ncs-2(tm1943) I; lite-1(ce314) X; juIs489[Punc-17-ChetaHR-mKate2]; juEx7119[Pacr-2-NCS-2(EFmut)-GFP]*	
CZ23855	*acr-16(ok789) V; juIs489[Punc-17-ChetaHR-mKate2]*	
CZ24146	*ncs-2(tm1943) I; acr-16(ok789) V; juIs489[Punc-17-ChetaHR-mKate2]*	
ZX426	*zxIs3[Punc-47-ChR2(H134R)-YFP] I*	Previously reported in (Liewald et al., 2008)
CZ15301	*zxIs3[Punc-47-ChR2(H134R)-YFP] I; acr-2(n2420) X*	
CZ22029	*juEx6678[Pacr-2-GCaMP6f-SL2-mKate2]*	
CZ22153	*acr-2(n2420) X; juEx6678[Pacr-2-GCaMP6f-SL2-mKate2]*	
CZ24971	*juIs517[Phsp-ACR-2(gf)]; juEx6678[Pacr-2-GCaMP6f-SL2-mKate2]*	
CZ22385	*ncs-2(tm1943) I; juEx6678[Pacr-2-GCaMP6f-SL2-mKate2]*	
CZ22386	*ncs-2(tm1943) I; acr-2(n2420) X; juEx6678[Pacr-2-GCaMP6f-SL2-mKate2]*	

CZ24882	*juEx6780[Pacr-2-NCS-2-GFP]*	
CZ24879	*juEx6935[Pacr-2-NCS-2(EFmut)-GFP]*	
CZ24938	*juEx6977[Pacr-2-NCS-2(G2A)-GFP]*	
CZ24941	*juEx6979[Pacr-2-NCS-2(S6F)-GFP]*	
CZ22351	*ncs-2(tm1943) I; acr-2(n2420) X; juEx6780[Pacr-2-NCS-2-GFP]*	multiple lines were visually observed for effects on *acr-2(gf)* induced behavior, and 2 lines were quantitated for convulsion frequency.
CZ22750	*ncs-2(tm1943) I; acr-2(n2420) X; juEx6935[Pacr-2-NCS-2(EFmut)-GFP]*	multiple lines were visually observed for effects on *acr-2(gf)* induced behavior, and 2 lines were quantitated for convulsion frequency.
CZ22861	*ncs-2(tm1943) I; acr-2(n2420) X; juEx6977[Pacr-2-NCS-2(G2A)-GFP]*	multiple lines were visually observed for effects on *acr-2(gf)* induced behavior, and 2 lines were quantitated for convulsion frequency.
CZ22863	*ncs-2(tm1943) I; acr-2(n2420) X; juEx6979[Pacr-2-NCS-2(S6F)-GFP]*	multiple lines were visually observed for effects on *acr-2(gf)* induced behavior, and 2 lines were quantitated for convulsion frequency.
CZ22777	*acr-2(ok1887) X; juEx6952[Phsp-ACR-2(gf)-GFP]*	*ok1887*: 2,857 bp deletion and 420 bp random nucleotide insertion in 5' region of K11G12.2, removes the first 3 exons of *acr-2* (Jospin et al., 2009)
CZ22917	*juEx6952[Phsp-ACR-2(gf)-GFP]*	
CZ24637	*juIs517[Phsp-ACR-2(gf)]*	
CZ24765	*ncs-2(tm1943) I; juIs517[Phsp-ACR-2(gf)]*	
CZ25297	*ncs-2(tm1943) I; juIs517[Phsp-ACR-2(gf)]; juEx7661[Pacr-2-NCS-2-GFP]*	
CZ25298	*ncs-2(tm1943) I; juIs517[Phsp-ACR-2(gf)]; juEx7662[Pacr-2-NCS-2(EFmut)-GFP]*	
CZ21292	*lgc-46(ju825gf) III; acr-2(n2420) X*	*ju825gf*: M314I in LGC-46 protein.
CZ21949	*acr-2(n2420) X; juEx6643[Punc-17β-LGC-46(gf)]*	

Table S2. Plasmid information, related to Figure 4, Figure 5 and Figure 7

Plasmid	Description	Description
PCZGY2671	*FRT-HygromycinR-FRT-Pncs-2-NCS-2-GFP*[a]	For Cas9-mediated insertion on Ch I (*ttTi4348*), it includes 4 kb upstream sequence from the start codon and 683 bp downstream sequence after stop codon of NCS-2.
PCZGY2673	*Prgef-1-NCS-2-GFP*	
PCZGY2674	*Pacr-2-NCS-2-GFP*	
PCZGY2675	*Punc-25-NCS-2-GFP*	
PCZGY2676	*Pncs-2-NCS-2-GFP*	
PCZGY2677	*Pacr-2-GCaMP6f-SL2-mKate2*	
PCZGY2678	*Pacr-2-NCS-2(EFmut)-GFP*	*EFmut: D75A/E86Q/D111A/E122Q/D158A/E169Q*
PCZGY2690	*Pacr-2-NCS-2(G2A)-GFP*	
PCZGY2694	*Punc-17β-NCS-2*	
PCZGY2762	*Pacr-2-NCS-2(S6F)-GFP*	
pCZGY3108	*Punc-17-ChetaHR-mKate2*	*ChetaHR: ChR2(E123T/ H134R)*
PCZ939	*Phsp-16.2-ACR-2(gf)-GFP*	
PCZ940	*Phsp-16.41-ACR-2(gf)-GFP*	
PCZ941	*Phsp-16.2-ACR-2(gf)*	
PCZ942	*Phsp-16.41-ACR-2(gf)*	

[a]: 3'*utr* of *ncs-2* is used for the construct. If not indicated, 3'*utr* of *unc-54* is used.

Supplemental Reference

Gendrel, M., Rapti, G., Richmond, J.E., and Bessereau, J.L. (2009). A secreted complement-control-related protein ensures acetylcholine receptor clustering. Nature 461, 992-996.

Jospin, M., Qi, Y.B., Stawicki, T.M., Boulin, T., Schuske, K.R., Horvitz, H.R., Bessereau, J.L., Jorgensen, E.M., and Jin, Y. (2009). A neuronal acetylcholine receptor regulates the balance of muscle excitation and inhibition in Caenorhabditis elegans. PLoS Biol 7, e1000265.

Liewald, J.F., Brauner, M., Stephens, G.J., Bouhours, M., Schultheis, C., Zhen, M., and Gottschalk, A. (2008). Optogenetic analysis of synaptic function. Nat Methods 5, 895-902.

Martin, J.A., Hu, Z., Fenz, K.M., Fernandez, J., and Dittman, J.S. (2011). Complexin has opposite effects on two modes of synaptic vesicle fusion. Curr Biol 21, 97-105.

Qi, Y.B., Po, M.D., Mac, P., Kawano, T., Jorgensen, E.M., Zhen, M., and Jin, Y. (2013). Hyperactivation of B-type motor neurons results in aberrant synchrony of the Caenorhabditis elegans motor circuit. J Neurosci 33, 5319-5325.